
Article:
Rozhnoi, A., Solovieva, M., Shalimov, S. et al. (6 more authors) (2020) The effect of the August 21, 2017 total solar eclipse on the phase of VLF/LF signals. Earth and Space Science, 7 (2). ISSN 2333-5084

https://doi.org/10.1029/2019ea000839

Earth and Space Science

RESEARCH ARTICLE
10.1029/2019EA000839

The Effect of the 21 August 2017 Total Solar Eclipse on the Phase of VLF/LF Signals

A. Rozhnoi[1], M. Solovieva[1], S. Shalimov[1,2], D. Ouzounov[3], P. Gallagher[4], G. Verth[5], J. McCauley[4], S. Shelyag[6], and V. Fedun[7]

[1]Schmidt Institute of Physics of the Earth, ,Moscow, Russian Federation, [2]Space Research Institute, Russian Academy of Sciences, Moscow, Russian Federation, [3]Schmid College of Science and Technology, Physics, Computational Science and Engineering, Chapman University, CA, USA, [4]Trinity College Dublin, University of Dublin, Dublin, Ireland, [5]Plasma Dynamics Group, School of Mathematics and Statistics, University of Sheffield, Sheffield, UK, [6]School of Information Technology, Deakin University, Geelong, Victoria, Australia, [7]Plasma Dynamics Group, Department of Automatic Control and Systems Engineering, University of Sheffield, Sheffield, UK

Key Points:
- Variations in phase of VLF/LF signals observed during a total solar eclipse of 21 August 2017 is analyzed
- Theoretically estimated variation of D region electron density coincide with observational results

Correspondence to:
V. Fedun,
v.fedun@sheffield.ac.uk

Citation:
Rozhnoi, A., Solovieva, M., Shalimov, S., Ouzounov, D., Gallagher, P., Verth, G., et al. (2019). The effect of the 21 August 2017 total solar eclipse on the phase of VLF/LF signals. *Earth and Space Science*. *6*. https://doi.org/10.1029/2019EA000839

Received 13 AUG 2019
Accepted 7 NOV 2019
Accepted article online 22 NOV 2019

Abstract An experimental study of the phase and amplitude observations of sub-ionospheric very low and low frequency (VLF/LF) signals is performed to analyze the response of the lower ionosphere during the 21 August 2017 total solar eclipse in the United States of America. Three different sub-ionospheric wave paths are investigated. The length of the paths varies from 2,200 to 6,400 km, and the signal frequencies are 21.4, 25.2, and 40.75 kHz. The two paths cross the region of the total eclipse, and the third path is in the region of 40–60% of obscuration. None of the signals reveal any noticeable amplitude changes during the eclipse, while negative phase anomalies (from −33° to −95°) are detected for all three paths. It is shown that the effective reflection height of the ionosphere in low and middle latitudes is increased by about 3–5 km during the eclipse. Estimation of the electron density change in the lower ionosphere caused by the eclipse, using linear recombination law, shows that the average decrease is by 2.1 to 4.5 times.

1. Introduction

The total solar eclipse on 21 August 2017, named the "Great American Eclipse," was observed within a narrow band (117 km) across the middle part of the United States from the Pacific to the Atlantic coasts (Figure 1). The first external contact of the penumbral shadow with Earth (point P1 in Figure 1) occurred at 15:46:51 UT to the north-east from the Hawaiian Islands and the last external contact (point P4 in Figure 1) took place at 21:04:23 UT near the northern coast of Brasilia. The total eclipse began at 16:48:36 UT and lasted until 20:02:34 UT.

The maximum eclipse had a duration of 160 s and occurred at the location with coordinates: 37°N 87.7°W starting at 18:26:40 UT. The partial solar eclipse was visible over a region thousands of kilometers wide from Canada to South America and partially in northwestern Europe and in the Chukchi Peninsula in Asia.

Solar eclipses give us unique possibility to study physical and chemical ionospheric processes when the solar radiation changes abruptly. They are also known to produce a decrease in the electron density in the ionosphere, a decrease in electron and ion temperature and a change in ionic composition in outer ionosphere (Rishbeth, 1968).

One of the few experimental techniques, which can be used to monitor ionization perturbations within lower ionosphere, is very low and low frequency (VLF/LF) radio wave probing. Such electromagnetic waves propagate in the lower ionosphere-Earth waveguide due to the reflection from the upper boundary (lower ionosphere at altitudes of $\approx$ 70 km in daytime and $\approx$ 90 km at nighttime) to the lower boundary (Earth surface) (Wait & Spices, 1964). Because of this, these waves inherently contain information about the reflection region of the ionosphere and its variability. The propagation of sub-ionospheric VLF signals over distances of thousands of kilometers enables remote sensing over large regions of the upper atmosphere in which ionospheric modifications lead to changes in the received amplitude and phase.

After the pioneering studies of Bracewell (1952), numerous observations of the phase and amplitude variations of sub-ionospheric signals in different frequency bands (10–60 kHz) during the solar eclipses were

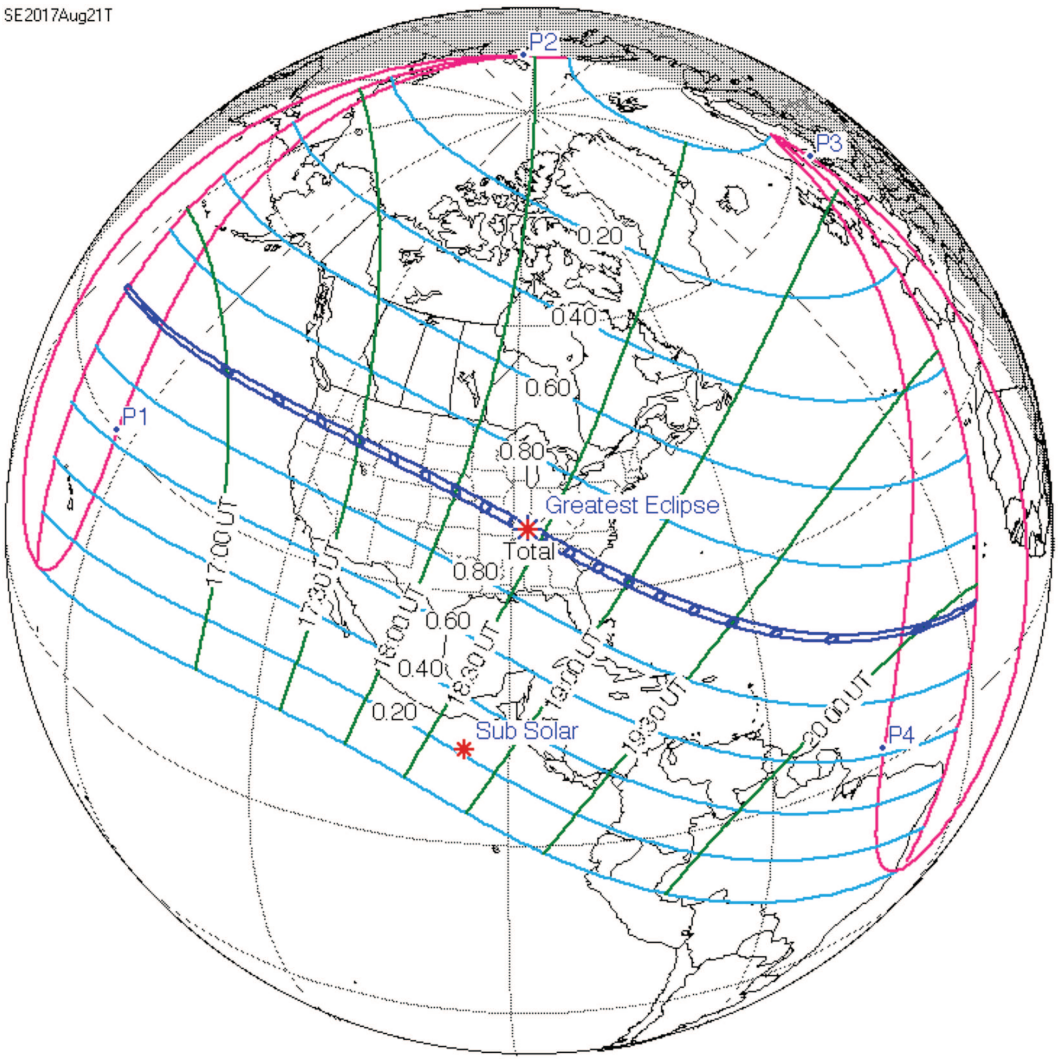

Figure 1. Solar eclipse on 21 August 2017 (https://eclipse.gsfc.nasa.gov/SEplot/SEplot2001/SE2017Aug21T.GIF). Double dark blue line shows the position of total eclipse. Light blue lines show positions of partial eclipses. Green lines indicate the time of the eclipse.

performed in the 1960s. These researchers examined a number of VLF transmitter signals along paths of different distances and orientations (Crary & Schneible, 1965; Hoy, 1969; Kamra & Varshneya, 1967; Kaufmann & Schaal, 1968).

In particular, these studies detailed the phase and amplitude perturbations associated with total or partial solar eclipses. It was found that the most effective method to monitor the variations of propagation characteristics is analysis of phase changes. Over paths of 1,000 to 10,000 km the amplitude was typically found to increase by about 1 dB, and the phase decreased by about 40°. Increases in the effective reflection height of the ionosphere were estimated to be between 6 and 11 km. Many authors (Gupta et al., 1980; Lynn, 1981; Mendes Da Costa et al., 1995; Reeve & Rycroft, 1972) suggested that ionospheric effects related to the solar eclipse depend on both the length of the path and the signal frequency.

Clilverd et al. (2001) studied in detail ionospheric effects during the total solar eclipse observed in Europe on 11 August 1999. The analysis of the amplitude and phase of four VLF transmitters in the frequency range 16–24 kHz was performed for 19 paths of different distances (from 90 to 14,510 km). Positive amplitude changes were observed on short paths, that is, less than 2,000 km, while negative amplitude changes were observed on longer paths, that is, more than 10,000 km. Negative phase changes were observed on most paths and were therefore independent of path length. The typical changes observed were 3 dB and 50°. These

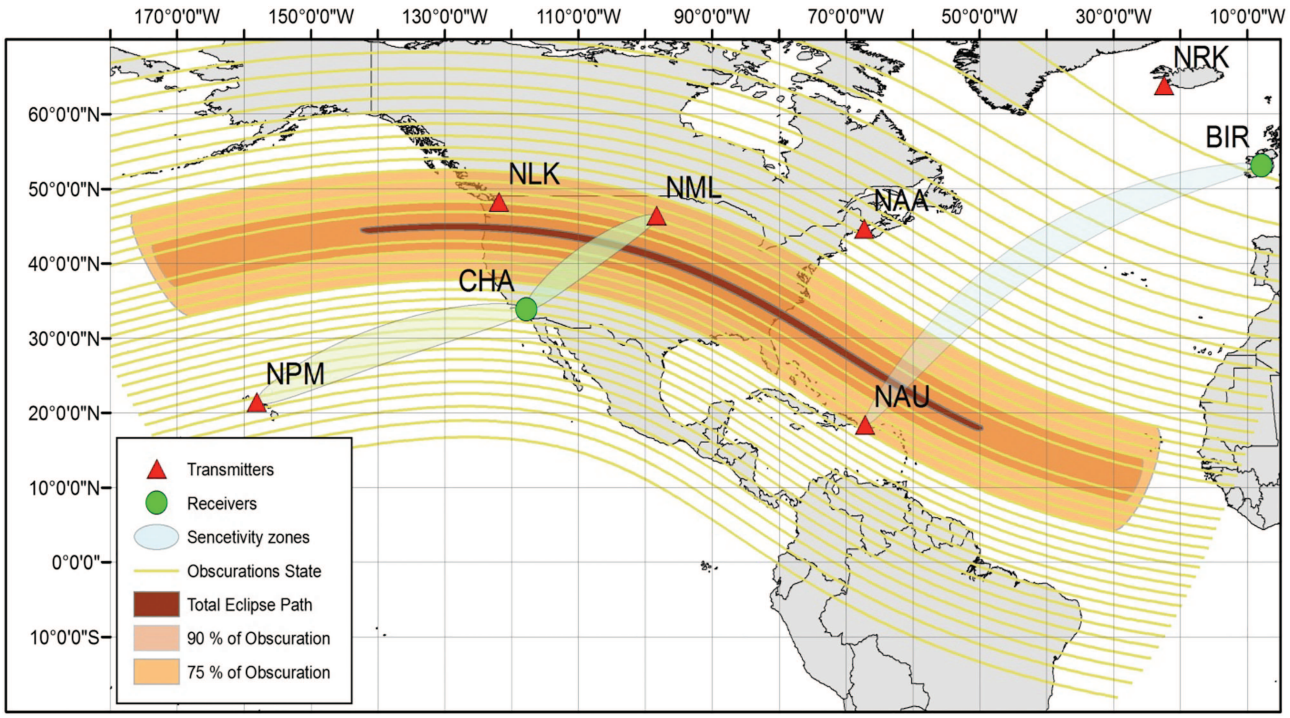

Figure 2. Relative positions of the receivers and transmitters together with the obscuration's degree (the last information t has been taken from: https://www.timeanddate.com/eclipse/solar/2017-august-21). The positions of the receivers in Birr, Ireland (BIR) and Orange, CA, USA (CHA) are shown by green circles. The positions of transmitters NPM (21.4 kHz), NML (25.2 kHz), and NAU (40.75 kHz) are shown by red triangles.

experimental results have been successfully modeled by taking into account chemical processes in the lower ionosphere.

In more recent works (see, e.g., De et al., 2011, 2011; Guha et al., 2010) the eclipse's effects on the equatorial lower ionosphere were reported for the total solar eclipse on 22 July 2009. The signals from different transmitters were registered in India. Analysis of the data confirmed that phase is a more sensitive characteristic than amplitude. It was found that during the eclipse, the effective reflection height of the ionosphere increased by 3 km.

In our previous work (Solovieva et al., 2016) we considered the amplitude and phase variations of VLF/LF signals (20–45 kHz) received in Moscow, Graz (Austria), and Sheffield (UK) during the total solar eclipse on 20 March 2015, in North West Europe. Four long paths crossed the 90–100% obscuration region, and the amplitude and phase anomalies were detected for all four paths. Negative phase anomalies varied from −75° to −90°, and the amplitude anomalies were both positive and negative. They did not exceed 5 dB. It was also found that the effective height of the ionosphere varied from 6.5 to 11 km during the eclipse.

Unlike previous works we found that the solar eclipse affected neither the signal frequency nor path length. Further experimental measurements of the ionospheric parameters at the time of solar eclipses are needed to understand this behavior and the characteristics of the ionosphere.

In the current work we use phase and amplitude observations of sub-ionospheric VLF/LF signals to analyze the response of the lower ionosphere to the Great American Eclipse on 21 August 2017. This eclipse has been analyzed in detail by Cohen et al. (2018) using observations from 11 VLF/LF receivers across the continental United States. Results of the analysis have shown increase in amplitude up to 5 dB during eclipse together with decrease in phase $\approx 10 - 50°$. No quantitative analysis of the ionospheric conditions during eclipse was made. Another work also presents the analysis of VLF signal during this eclipse (Moore & Burch, 2018). These authors observed both amplitude and phase on many

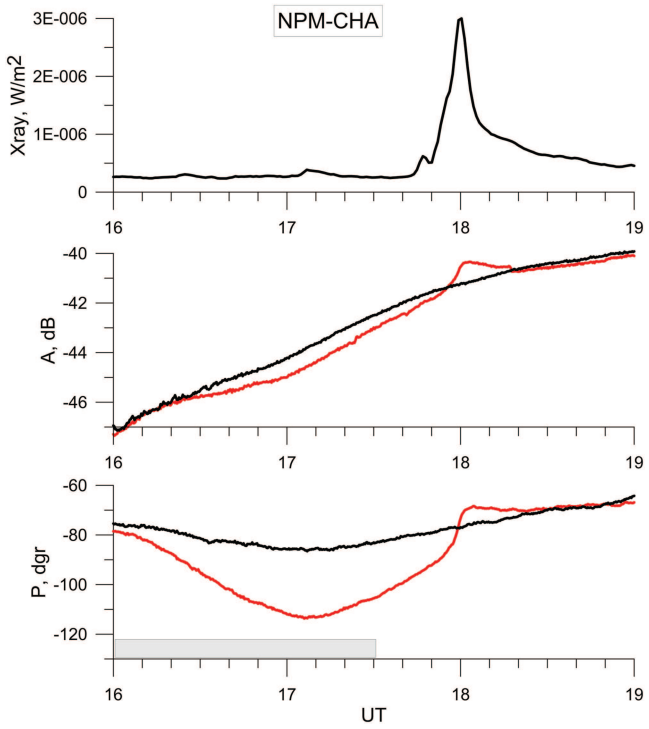

Figure 3. Results of the analysis for wave path NPM-CHA. Top panel shows X-ray flux measured with the GOES 14 satellite in the wavelength range of 0.1–0.8 nm. Middle panel shows the amplitude variations on 21 August 2017 (red) and its monthly averaged values (black). Bottom panel shows phase variations on 21 August 2017 (red) and its monthly averaged values (black). Gray rectangles along the time axes show period when a large part of the path has been obscured.

middle length VLF paths from NLM transmitter. They reported a change in amplitude of $\approx 1-6$ dB and a change in phase from $-10°$ to $-50°$.

2. Data Description and Analysis

For analysis of sub-ionospheric VLF/LF perturbations caused by the Great Solar Eclipse we used measurements of ground-based UltraMSK receiving stations installed at the Chapman University, Orange, CA, USA (CHA) and Birr, Ireland (BIR). These receivers have been developed by Dr James Brundell, University of Otago, New Zealand. They can simultaneously record both the phase and amplitude of MSK (Minimum Shift Key) modulated signals in the frequency range 10–50 kHz from several VLF/LF transmitters. MSK signals have fixed frequencies in a narrow band of 200 Hz around the main frequency with adequate phase stability. The receiver station consists of a VLF antenna with a preamplifier, GPS receiver with a GPS antenna for accurate signal timing, an analog-to-digital converter, and a computer with specialized software. The receiver can record signals with time resolutions ranging from 50 ms to 60 s. More details are available at http://ultramsk.com/. For our purpose we use a sampling frequency of 20 s. The locations of the receivers and transmitters are shown in Figure 2. Three of them were used in the present study: NML (La Moure, North Dakota, USA), NPM (Pearl Harbor, Hawaii, USA), and NAU (Aguadu, Puerto Rico).

Unfortunately, during this solar eclipse, the most powerful transmitter (NAA, Cutler, Maine, frequency 24 kHz) was inactive. Additionally, we did not use the phase measurements of the NLK (24.8 kHz) and NAU (40.75 kHz) signals in CHA station because of unstable phase reception in this station. The NML and NLK signals were not received in Birr, and NPM signals were too weak for reliable analysis.

Therefore we selected only three sub-ionospheric paths, namely NPM-CHA, NML-CHA, and NAU-BIR (see Figure 2). The location of transmitter-receiver pairs enabled us to monitor the region from Hawaii, through North America, and on to Puerto Rico.

The results of the analysis are shown in Figures 3–5. In comparison to our previous study (Solovieva et al., 2016) none of the signals received during the eclipse revealed any noticeable changes in the amplitude. Figure 3 shows the amplitude and phase variations on 21 August 2017 (in red color) and the monthly averaged values (in black color). Small decrease (about 1 dB) of the NPM signal amplitude can be seen in Figure 3. Note, the decrease in the amplitude is within the standard deviation of the signal for quiet days. For the two other paths the amplitudes of signals are rather noisy, and it is impossible to identify any effects. Next we describe the results of the analysis on the three different paths, NPM-CHA, NML-CHA, and NAU-BIR, separately.

First we consider the NPM-CHA path which has an approximate length of about 4,000 km and is in the region of 40–60% of obscuration (see Figure 1). On this path the observed partial phase of the total eclipse started at 15:46 UT. From Figure 3 (bottom panel), it can be seen that just after 17:00 UT the eclipse reached the receiver (this period is shown by the gray rectangle along the time axis). At 18:00 UT (at the time of the solar X-ray flare of C3 class was registered by geostationary satellite the GOES 14) the whole path was sunlit. Both in the phase and amplitude of signal the effect of the solar flare is clearly visible. Thereafter, signal returns to its normal level. The maximum phase decrease in the NPM-CHA path was observed between 17:00 and 17:15 UT when practically the whole path was obscured and the phase deviated from its normal level by 33°.

The next wave path, MML-CHA, which is actually on the total eclipse path, has a length of about 2,200 km. Results of the analysis for this particular path are shown in Figure 4. The top panel corresponds to the measured X-ray flux detected by GOES 14 satellite in the wavelength range of 0.1–0.8 nm. The bottom panel

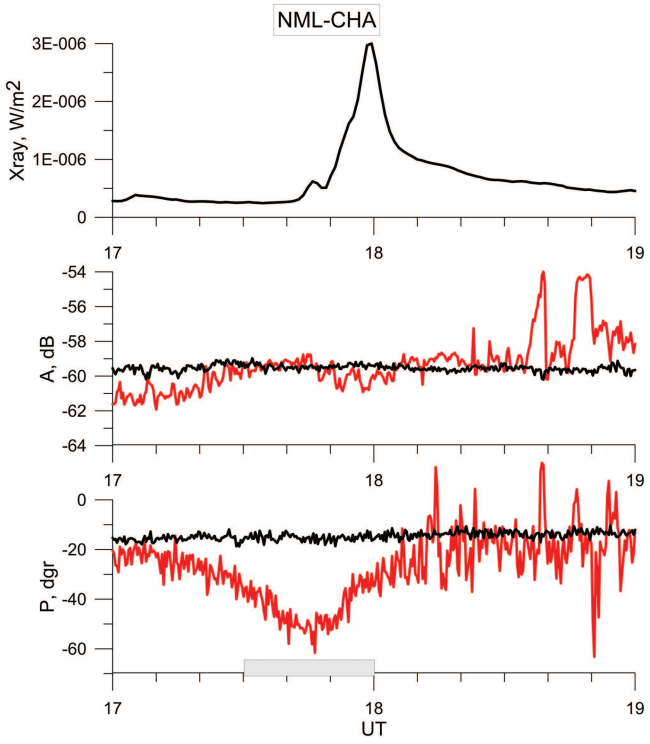

Figure 4. Results of the amplitude and phase analysis for wave path NML-CHA. Explanations are the same as in Figure 3.

shows phase variations on 21 August 2017 (red) and its monthly averaged values (black). It is important to note that the NML transmitter for this is located in the region of 80% obscuration and the CHA receiver is in the area of 60% of obscuration. For this path the eclipse reached the receiver and transmitter at 17:30 and 18:00 UT, respectively. The gray rectangle along the time axis marks this interval (see Figure 4). The signal crossed the region of 90–100% obscuration at approximately 17:45–17:50 UT. This is at the same time as we can see the maximum drop in the phase of VLF signal. The recorded phase change is about −35°, and it took only 20 min for a full phase recovery. The effect from the solar flare at 18 UT is not noticeable in this signal. The amplitude oscillates chaotically. The oscillations are inside dispersion boundaries.

Finally we analyze the phase and amplitude changes along the NAU-BIR path (Figure 5). This path has a length of about 6,400 km and crosses the region with 90–100% obscuration. This rather long path has a sub-meridional orientation and it is obscured for a relatively short period of time, that is, between 19:10 UT till 19:40 UT. The maximum decrease in the phase is observed during the maximum obscuration around 19:30 UT. The phase decrease of 95° is more than for the other two paths, NPM-CHA and MML-CHA. This could be related to the greater length of NAU-BIR path, the different orientation of the geomagnetic field or, most probably, the higher LF signal frequency. In this case the phase recovered about 1 hr after the signal dropping. The amplitude oscillates chaotically and, therefore, it is difficult to identify effects caused by the eclipse. The oscillations are inside dispersion boundaries.

It should be also mentioned that the magnetic activity was rather low during 21 August ($Dst < -20$ nT). Therefore, the observed anomalies in the VLF signals cannot be attributed or explained by influence of the geomagnetic environment.

Our explanation of the effect of the solar eclipse on phase of VLF/LF signals is as follows. It is known that ionization of the ionosphere strongly depends on the solar activity. Ultraviolet and X-ray radiation dominate the ionization processes during the day but disappear above solar eclipse region. As a result, the ionization of the D region significantly decreases. This process leads to an increase of the effective reflection height of the ionosphere. As the transmitted signals propagate within the Earth-ionosphere waveguide, the propagation paths of the VLF/LF signals increase in length, and this is responsible for the observed phase delay of the sub-ionospheric signals. The phase delay due to an increase in reflection height can be determined as (Pant & Mahra, 1994)

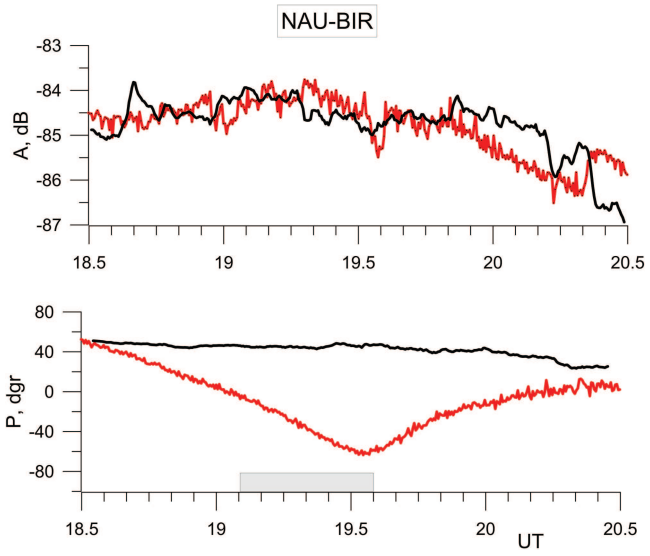

Figure 5. Results of the amplitude and phase analysis for wave path NAU-BIR. Explanations are the same as in Figure 3.

$$\Delta\varphi = 2\pi\frac{d}{\lambda}\left(\frac{1}{2a} + \frac{\lambda^2}{16h^3}\right)\Delta h, \quad (1)$$

where d is distance between transmitter and receiver in km, λ is wavelength of signal in km, a is radius of the Earth, h is the reflection height, and Δh is increase in reflection height. From this it follows that the increase in reflection height is

$$\Delta h = \frac{\Delta\varphi}{2\pi\frac{d}{\lambda}\left(\frac{1}{2a} + \frac{\lambda^2}{16h^3}\right)}. \quad (2)$$

Using the obtained experimental values of $\Delta\varphi$ and by taking as $h = 70$ km, we found that Δh for path NPM-CHA was 2.67 km, for path NML-CHA it was $\approx$ 5.1 km, and for path NAU-BIR the increase in

reflection height was ≈ 3.4 km. These results are in a good agreement with the data obtained previously by De et al. (2011) and Guha et al. (2010) for low latitudes.

3. Estimates of Electron Density Change

Due to the relatively short lifetime of the ions in the lower ionosphere, a steady-state computation of the electron density provides an adequate description over a wide range of conditions, so that electron density N_e can be considered to be the result of an equilibrium between ion production rate, q, and effective electron loss. There exist two approaches regarding the electron loss in the D region, which we consider now, namely, the quadratic recombination law (Chernogor et al., 2019) and the linear recombination law (Belikovich et al., 2006). Introducing the ratio (eclipse obscuration) S_1/S_0, where S_1, S_0 are the shaded part of the Sun's disk and the area of the Sun's disk, respectively; one may estimate the ion production rate as $q_1 = q_0\left(1 - S_1/S_0\right)$, where q_1, q_0 are the disturbed ionization rate and the ionization rate in the absence of an eclipse, respectively.

Therefore, in case of the quadratic recombination law $q = \alpha n^2$, where n is the electron density, we obtain

$$\frac{n_1}{n_0} = \sqrt{\frac{\alpha_0}{\alpha_1}\left(1 - \frac{S_1}{S_0}\right)}, \tag{3}$$

where α_0, α_1 are the recombination coefficient in the absence of an eclipse and disturbed recombination coefficient, and n_0, n_1 are the undisturbed and disturbed electron density, respectively. On the other hand, in case of the linear recombination law $q = \gamma n$ one obtains

$$\frac{n_1}{n_0} = \frac{\gamma_0}{\gamma_1}\left(1 - \frac{S_1}{S_0}\right). \tag{4}$$

Now we use the calculated obscurations (https://eclipse.gsfc.nasa.gov/SEgoogle/SEgoogle2001/SE2017Aug21Tgoogle.html) for the three different paths. For the path NML-CHA the ratio S_1/S_0 varies from 0.56 to 1, with an average value equal to 0.78. Putting in our estimates $\alpha_0 \approx \alpha_1$, $\gamma_0 \approx \gamma_1$ we obtain from equation (3) $n_1/n_0 \approx 0.47$ and from equation (4) $n_1/n_0 \approx 0.22$. This corresponds to $\Delta n/n_0 = 0.53$ in the former case and to $\Delta n/n_0 = 0.78$ in the latter case. Accordingly, the average decrease of the electron density along the path is 2.1 and 4.5 times.

Let us estimate the electron density change during the eclipse in another way. For that we assume a linear profile of the electron density in the vicinity of the radio wave reflection height. This yields the following expression

$$\frac{\Delta n}{n_0} = \frac{n_1 - n_0}{n_0} = \frac{\Delta h}{H}, \tag{5}$$

where Δh is the change of the reflection height due to the eclipse, and H is the characteristic scale of the electron density profile. The change in the reflection height can be determined from equation (2). For this path, using equation (2), $\Delta h \approx 5.1$ km with $H = 6.5$ km (Whitten & Poppoff, 1971), and equation (5) gives $\Delta n/n_0 = 0.78$. This corresponds well to our previous estimate with the linear recombination rate.

Likewise, assuming linear recombination rates for paths NPM-CHA and NAU-BIR the average S_1/S_0 ratio for these paths is 0.4 and 0.53, respectively. So, again using equation (4) we obtain $n_1/n_0 \approx 0.60$ for the first path which corresponds to $\Delta n/n_0 = 0.40$ and $n_1/n_0 \approx 0.47$ for the second path which corresponds to $\Delta n/n_0 = 0.53$.

On the other hand, we may estimate the quantity $\Delta n/n_0$ using equation (5). Taking calculated value Δh for the path NPM-CHA as $\Delta h \approx 2.67$ km and for the path NAU-BIR as $\Delta h \approx 3.4$ km with $H = 6.5$ km we obtain from equation (5) that $\Delta n/n_0 = 0.41$, $\Delta n/n_0 = 0.53$ for these paths, respectively. These values are in good agreement with our previous estimates assuming a linear recombination rate.

4. Conclusions

In this work we present VLF/LF observations of the phase and amplitude of three sub-ionospheric wave paths during the total solar eclipse of 21 August 2017. The length of these paths varied from 2,200 to 6,400

km, signal frequencies were 21.4, 25.2, and 40.75 kHz, and obscuration along the paths was different. Two sub-ionospheric paths crossed the total eclipse path, and the third path was in the region of 40–60% of obscuration. We found that for all three paths there was no noticeable influence on amplitude; however, the phase revealed a significant decrease during the eclipse. For the two signals transmitted from NPM and NML transmitters which both had frequencies close to 20 kHz the negative phase anomalies were −33° and −35°, correspondingly, which is in good agreement with the experimental results, obtained by Cohen et al. (2018) and Moore and Burch (2018) for the American paths. Note that the anomalies lasted longer for the longer path. The strongest decrease in phase was found for the wave path NAU-BIR (−95°). For the same path the time duration of anomalies also lasted the longest.

These results, again, confirm that the effect of solar eclipses are more distinct in the phase of VLF/LF signals (Guha et al., 2010; Hoy, 1969; Kaufmann & Schaal, 1968). Although previous works have reported very small (≈ 1 dB) amplitude variations during solar eclipses such variations in our measurements are invisible against background oscillations, that is, they are comparable with measurement error.

It was also found that the effective reflection height of the ionosphere in low and middle latitudes increased by about 3–5 km during the eclipse. An estimation of the electron density change in the lower ionosphere during the eclipse was made using two different assumptions regarding the electron loss in the D region, that is, the quadratic recombination law and the linear recombination law. The values obtained were in good agreement and showed that the average decrease was between 2.1 to 4.5 times.

Acknowledgments
RAW data of the VLF observations are available at ORDA - The University of Sheffield Research Data Catalogue and Repository (https://orda.shef.ac.uk/). VF and GV are grateful to the Royal Society, International Exchanges Scheme - 2017/R1 Standard Programme Grant IE170301 and International Exchanges Scheme - 2019/R1 Standard Programme Grant IES/R1/191114. Also, VF thanks for support the Science and Technology Facilities Council (STFC) Grant ST/M000826, the Natural Environment Research Council (NERC) Grant NE/P017061/1, and the Air Force Office of Scientific Research (USA) Grant 18IOA009.

References

Belikovich, V. V., Vyakhirev, V. D., Kalinina, E. E., Tereshchenko, V. D., Ogloblina, O. F., & Tereshchenko, V. A. (2006). Studies of the ionospheric D-region using partial reflections in spring 2004 at middle and high latitudes. *Geomagnetism and Aeronomy*, *46*, 218–221. https://doi.org/10.1134/S0016793206020113

Bracewell, R. N. (1952). Theory of formation of an ionospheric layer below E layer based on eclipse and solar flare effects at 16 kc/sec. *Journal of Atmospheric and Terrestrial Physics*, *2*, 226–235. https://doi.org/10.1016/0021-9169(52)90033-0

Chernogor, L. F., Domnin, I. F., Emelyanov, L. Y., & Lyashenko, M. V. (2019). Physical processes in the ionosphere during the solar eclipse on March 20, 2015 over Kharkiv, Ukraine (49.6 N, 36.3 E). *Journal of Atmospheric and Solar-Terrestrial Physics*, *182*, 1–9. https://doi.org/10.1016/j.jastp.2018.10.016

Cohen, M. B., Gross, N. C., Higginson-Rollins, M. A., Marshall, R. A., Gołkowski, M., Liles, W., et al. (2018). The lower ionospheric VLF/LF response to the 2017 Great American Solar Eclipse observed across the continent. *Geophysical Research Letters*, *45*, 3348–3355. https://doi.org/10.1002/2018GL077351

Crary, J. H., & Schneible, D. E. (1965). Effect of the solar eclipse of 20 July 1963 on VLF signal propagating over short paths. *Radio Science*, *69*, 947–957.

De, K. B., De, S. S., Bandyopadhyay, B., Pal, P., Ali, R., Paul, S., & Goswami, P. K. (2011). Effects of a solar eclipse on the propagation of VLF-LF signals: Observations and results. *Terrestrial, Atmospheric and Oceanic Sciences*, *22*, 435–442. https://doi.org/10.3319/TAO.2011.01.17.01(AA)

De, S. S., De, B. K., Bandyopadhyay, B., Paul, S., Barui, S., Haldar, D. K., et al. (2011). Effects of solar eclipse on long path VLF transmission. *Bulgarian Journal of Physics*, *38*, 206–215.

Guha, A., de, B. K., Roy, R., & Choudhury, A. (2010). Response of the equatorial lower ionosphere to the total solar eclipse of 22 July 2009 during sunrise transition period studied using VLF signal. *Journal of Geophysical Research*, *115*, A11302. https://doi.org/10.1029/2009JA015101

Gupta, A. S., Goel, G. K., & Mathur, B. S. (1980). Effect of the 16 February 1980 solar eclipse on VLF propagation. *Journal of Atmospheric and Terrestrial Physics*, *42*, 907–909.

Hoy, R. D. (1969). The effect of a total solar eclipse on the phase of long path v.l.f. transmissions. *Journal of Atmospheric and Terrestrial Physics*, *31*, 1027–1028. https://doi.org/10.1016/0021-9169(69)90149-4

Kamra, A. K., & Varshneya, N. C. (1967). The effect of a solar eclipse on atmospheric potential gradients. *Journal of Atmospheric and Terrestrial Physics*, *29*, 327–329. https://doi.org/10.1016/0021-9169(67)90204-8

Kaufmann, P., & Schaal, R. E. (1968). The effect of a total solar eclipse on long path VLF transmission. *Journal of Atmospheric and Terrestrial Physics*, *30*, 469–471. https://doi.org/10.1016/0021-9169(68)90119-0

Lynn, K. J. W. (1981). The total solar eclipse of 23 October 1976 observed at VLF. *Journal of Atmospheric and Terrestrial Physics*, *43*, 1309–1316. https://doi.org/10.1016/0021-9169(81)90156-2

Mendes Da Costa, A., Paes Leme, N. M., & Rizzo Piazza, L. (1995). Lower ionosphere effect observed during the 30 June 1992 total solar eclipse. *Journal of Atmospheric and Terrestrial Physics*, *57*, 13–17. https://doi.org/10.1016/0021-9169(93)E0021-Z

Moore, R. C., & Burch, H. C. (2018). The D region response to the August 2017 total solar eclipse and coincident solar flare. *Geophysical Research Letters*, *45*, 13,192–13,198. https://doi.org/10.1029/2018GL080762

Pant, P., & Mahra, H. S. (1994). Effect of solar eclipses on VLF propagation. *Indian Journal of Radio & Space Physics*, *23*, 399–402.

Reeve, C. D., & Rycroft, M. J. (1972). The eclipsed lower ionosphere as investigated by natural very low frequency radio signals. *Journal of Atmospheric and Terrestrial Physics*, *34*, 667–672. https://doi.org/10.1016/0021-9169(72)90154-7

Rishbeth, H. (1968). Solar eclipses and ionospheric theory. *Space Science Review*, *8*, 543–554. https://doi.org/10.1007/BF00175006

Solovieva, M. S., Rozhnoi, A. A., Fedun, V., & Schwingenschuh, K. (2016). Effect of the total solar eclipse of March 20, 2015, on VLF/LF propagation. *Geomagnetism and Aeronomy*, *56*, 323–330. https://doi.org/10.1134/S0016793216030166

Wait, J. R., & Spices, K. P. (1964). Characteristics of the Earth ionosphere waveguide for VLF radio waves. *NBS Tech. Note*, 300.

Whitten, R. C., & Poppoff, I. G. (1971). Fundamentals of aeronomy.